






Review

Recent Advances in Inflammatory Diagnosis with Graphene Quantum Dots Enhanced SERS Detection

Seyyed Mojtaba Mousavi ^{1,*}, Seyyed Alireza Hashemi ², Masoomeh Yari Kalashgrani ³, Darwin Kurniawan ¹, Ahmad Gholami ³, Vahid Rahmanian ⁴, Navid Omidifar ⁵ and Wei-Hung Chiang ^{1,*}

¹ Department of Chemical Engineering, National Taiwan University of Science and Technology, Taipei City 106335, Taiwan; jdkywt@gmail.com

² Nanomaterials and Polymer Nanocomposites Laboratory, School of Engineering, University of British Columbia, Kelowna, BC V1V 1V7, Canada; s.a.hashemi0@gmail.com

³ Biotechnology Research Center, Shiraz University of Medical Science, Shiraz 71468-64685, Iran; masoomeh.yari.72@gmail.com (M.Y.K.); gholami@sums.ac.ir (A.G.)

⁴ Centre of Molecular and Macromolecular Studies, Polish Academy of Sciences, Sienkiewicza 112, 90-363 Lodz, Poland; vahid_rahmanian@live.com

⁵ Department of Pathology, School of Medicine, Shiraz University of Medical Sciences, Shiraz 71468-64685, Iran; omidifarn@sums.ac.ir

* Correspondence: mousavi.nano@gmail.com (S.M.M.); whchiang@mail.ntust.edu.tw (W.-H.C.)

Abstract: Inflammatory diseases are some of the most common diseases in different parts of the world. So far, most attention has been paid to the role of environmental factors in the inflammatory process. The diagnosis of inflammatory changes is an important goal for the timely diagnosis and treatment of various metastatic, autoimmune, and infectious diseases. Graphene quantum dots (GQDs) can be used for the diagnosis of inflammation due to their excellent properties, such as high biocompatibility, low toxicity, high stability, and specific surface area. Additionally, surface-enhanced Raman spectroscopy (SERS) allows the very sensitive structural detection of analytes at low concentrations by amplifying electromagnetic fields generated by the excitation of localized surface plasmons. In recent years, the use of graphene quantum dots amplified by SERS has increased for the diagnosis of inflammation. The known advantages of graphene quantum dots SERS include non-destructive analysis methods, sensitivity and specificity, and the generation of narrow spectral bands characteristic of the molecular components present, which have led to their increased application. In this article, we review recent advances in the diagnosis of inflammation using graphene quantum dots and their improved detection of SERS. In this review study, the graphene quantum dots synthesis method, bioactivation method, inflammatory biomarkers, plasma synthesis of GQDs and SERS GQD are investigated. Finally, the detection mechanisms of SERS and the detection of inflammation are presented.

Keywords: inflammatory; graphene quantum dots; SERS; detection



Citation: Mousavi, S.M.; Hashemi, S.A.; Yari Kalashgrani, M.; Kurniawan, D.; Gholami, A.; Rahmanian, V.; Omidifar, N.; Chiang, W.-H. Recent Advances in Inflammatory Diagnosis with Graphene Quantum Dots Enhanced SERS Detection. *Biosensors* **2022**, *12*, 461. <https://doi.org/10.3390/bios12070461>

Received: 28 May 2022

Accepted: 21 June 2022

Published: 27 June 2022

Publisher's Note: MDPI stays neutral with regard to jurisdictional claims in published maps and institutional affiliations.



Copyright: © 2022 by the authors. Licensee MDPI, Basel, Switzerland. This article is an open access article distributed under the terms and conditions of the Creative Commons Attribution (CC BY) license (<https://creativecommons.org/licenses/by/4.0/>).

1. Introduction

When tissue is damaged by bacteria, trauma, chemicals, heat, or other phenomena, several substances are released from the damaged tissue that cause very serious secondary changes in the tissue. This series of tissue changes is called inflammation. Inflammation is basically a protective response that fights the cause of cellular damage (e.g., germs or toxins) and the consequences of that damage, i.e., necrotic cells and tissues [1–4]. Inflammation causes hypersensitivity reactions to insect bites, drugs, and toxins, as well as some chronic diseases, such as rheumatoid arthritis, atherosclerosis, and pulmonary fibrosis [5–8]. Inflammation is a complex process that begins with tissue damage caused by endogenous factors, such as tissue necrosis and bone fractures, or exogenous factors, such as mechanical, physical, biological damage (like infection with microorganisms or

immunological responses, such as hypersensitivity reactions), and is accompanied by the invasion of inflammatory cells into the inflamed area [9,10]. Graphene quantum dots are a new generation of quantum dot structures. This new generation of carbon compounds contains a large number of functional groups and is synthesised in very small dimensions that exhibit a variety of other properties of carbon-based materials. Graphene quantum dots generally have a sheet structure of less than 10 nm in size and have received much attention in recent years due to their unique chemical and physical properties [11,12]. Compared with semiconductor quantum dots, graphene quantum dots are characterised by high water solubility, good photoluminescence properties, biocompatibility, optimal accessibility, easy surface functionalization, high stability, and low toxicity [13,14]. Thus, GQDs effectively reduce hyperinflammation by regulating immune cells, suggesting that they can be used as promising diagnostic agents to diagnose inflammation [15,16]. Surface-enhanced Raman spectroscopy (SERS) has also attracted great interest in various fields, such as medicine and analytical chemistry, due to its unique properties—sensitivity to single molecules on the surface, multiplexing potential, and fingerprinting capabilities [17–20]. One of the most important substrates of SERS, which includes quantum dots, has a wide range of applications in inflammation diagnosis, biological and chemical imaging, and labelling due to the plasmonic resonance properties of the surface-dependent local area, the chemical richness of the core-shell, and the compatible size [21–25]. In addition, graphene quantum dots also serve as a building block for an atomically flat SERS substrate, in which a much more uniform Raman signal can be obtained [26–28]. Graphene quantum dots (GQDs) have more accessible edges and larger specific surface areas than conventional graphene sheets, resulting in more efficient adsorption of target molecules [29–31].

This review study aims to explore recent advances in inflammation diagnostics using graphene quantum dots to improve the detection of SERS and highlight future areas of work in this field. In addition, the graphene quantum dots, bioactivation method, GQD synthesis method, inflammation biomarkers, plasma synthesis of GQDs, and SERS GQD were investigated. In addition, the detection methods of SERS and the detection of pro-inflammatory substances were evaluated.

2. Graphene Quantum Dot

Graphene quantum dots have attracted the attention of many researchers due to the crystalline structure of a single or a small amount of crushed graphene. These nanoparticles are a small lattice structure of honeycombs of carbon atoms that are less than 10 nanometers in size. Graphene quantum dots (GQDs) are, by definition, a type of quantum dot material with a graphene-derived property and carbon dots that can be placed in the form of very small graphene pieces (Figure 1). The carbon dots exhibit strong optical absorption in the UV region (260–320 nm) with an extended sequence in the visible and infrared regions. In addition, GQDs are semiconductor quantum dots with excellent light stability, biocompatibility and low toxicity, good electron mobility and good chemical stability, small size, electrochemical luminescence, photocatalyst capabilities, and are suitable for the fabrication of multiple sensors and bioimaging [32–36]. GQDs are less toxic than graphene oxides and have no obvious toxicity in the body, so GQDs have attracted much attention in biological applications, especially in the field of biopharmaceuticals [37,38]. Numerous groups have explored recent advances in graphene quantum dots for the construction of various sensors, including electron sensors, photoluminescence sensors (PL), electrochemical sensors, electrochemical luminescence sensors, PL-based high-conversion sensors, and surface-enhanced Raman spectroscopy (SERS) [39–42]. GQDs have become a prominent substance for the design of SERS due to their outstanding properties and model assumptions, such as high electron transfer rate, higher biomolecule loading, fast transduction, larger surface areas, easy surface functionalization, and inimitable electrocatalytic properties. These GQD enhanced SERS have been utilised for the detection of nucleic acids, amino acids, bioflavonoids, vitamins, small molecules, biomarkers, and heavy metal ions with remarkable properties [43].

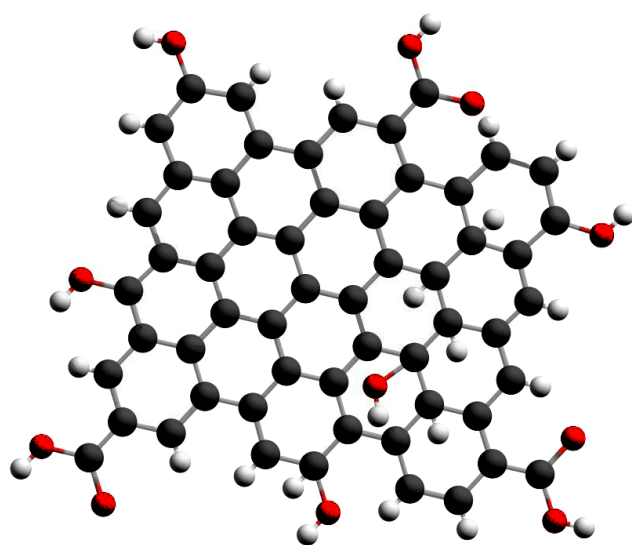


Figure 1. Graphene quantum dot. (●: Carbon, ●: Hydrogen, ●: Oxygen).

2.1. Method of Synthesis GQD

Graphene quantum dots are synthesized to optimize the size of quantum dots by two methods: top-down and bottom-up (Figure 2). In the top-down method, bulky carbon, graphite, and graphene materials are converted into graphene quantum dots, while in the bottom-up method, organic molecules are used as the carbon source. The disadvantages of the top-down method are the difficulties in controlling the size distribution and morphology of the produced particles. In contrast, the properties of the produced nanoparticles can be well controlled by the bottom-up method. In general, the optical properties of graphene nanodots depend on the size and the effect of quantum confinement, which changes the density and the nature of sp^2 sites. Therefore, the energy of these nanoparticles changes with the size of the gap [44–47]. Functionalizing the surface and doping the GQDs with other elements are other possible strategies to change these energy gaps while increasing the photoluminescence quantum yield (PLQY) of the GQDs by suppressing the emitting traps.

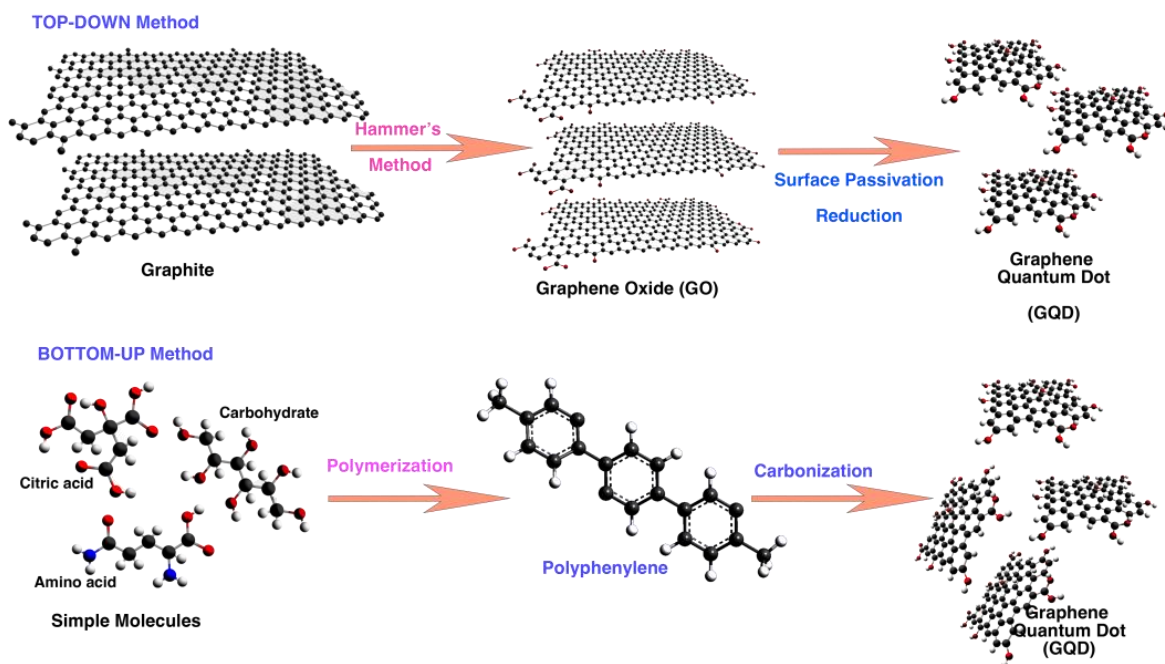


Figure 2. Schematic diagram representing the top-down and bottom-up approaches for the synthesis of GQDs.

In the top-down method, coal, which is considered the cheapest and easiest material to cleave compared to the other available materials, is exfoliated to form GQDs. For example, Ye et al. first sonicated coal in a mixture of concentrated sulfuric acid and nitric acid for 2 h before heat-treating the mixture in an oil bath at 100–120 °C for 24 h to produce GQDs [48]. Yan et al. succeeded in controlling the band gap of the coal-derived GQDs using a surface functionalization technique. In the typical procedure, the coal-derived GQDs were mixed in a toluene solution with various organic compounds (e.g., *o*-phenylenediamine, 2,3-diaminonaphthalene, 1,8-diaminonaphthalene, 1,1'-bi(2-naphthylamine), *p*-anisidine, 4-(trifluoromethoxy)-aniline, or 4-(trichloromethoxy)-aniline) and then solvothermally treated at 180 °C for 12 h to systematically adjust the band gap of the GQDs [49]. Since there are many concerns about the use of strong concentrated acids, Shin et al. prepared GQDs from various natural carbon sources using an acid-free oxone oxidant-assisted solvothermal technique [50]. Another acid-free strategy based on the ultrasonic irradiation of a mixture of anthracite charcoal and *N,N*-dimethylformamide (DMF) was used by Zhang et al. to prepare GQDs [51]. Since most of the feedstocks used are non-renewable sources and sometimes special chemicals are required to obtain GQDs with tunable emissions, and since high temperatures and long reaction times are also required, the feasibility of the top-down method is significantly hindered, especially when addressing the current problem of global energy limitations.

In contrast, the bottom-up method uses polycyclic aromatic compounds or other molecules with an aromatic structure, such as fluorene [25,52–55]. Table 1 shows the characteristics of the top-down and bottom-up methods in the synthesis of GQDs. However, the toxicity of these aromatic precursors may have a negative impact on the environment and is therefore considered unsuitable for large-scale production. For this reason, many efforts have been made to utilize naturally available biomasses as the main starting materials for the synthesis of GQDs. Citric acid, as one of the most commonly used biomasses, can be pyrolyzed directly at 200 °C to obtain blue-emitting GQDs [56]. Nitrogen-containing molecules can be used, together with citric acid, to prepare readily nitrogen-doped GQDs (NGQDs). Wu et al. synthesized blue-emitting NGQDs with a PLQY of 36.5% from a mixture of citric acid and dicyandiamide using a hydrothermal technique at 180 °C for 3 h [57]. Recently, biomass waste has attracted much attention due to its low cost, renewable and environmentally friendly properties. Kumar et al. reported a one-step preparation of NGQDs from chitosan using a chemical vapor deposition (CVD) system at 250–300 °C [58]. To avoid the use of high temperatures, Chiang's group used microplasma technologies to synthesize colloidal NGQDs with a PLQY of 30% from chitosan at ambient conditions [59]. Various strategies involving plasma flow, reaction time, and the type of acid used to dissolve chitosan were employed to control the functionalities and thus the energy gap of the resulting NGQDs [59,60]. Another promising biomass waste as a GQD precursor is lignin, which consists of phenyl skeletons and oxygenated branches [61]. Unlike simple structures, such as citric acid and glucose, both chitosan and lignin are biopolymers with complex structures, so the synthesis mechanism could involve a combination of top-down and bottom-up processes. The underlying mechanism is thought to consist of two main steps. These include the decomposition of long-chain structures into smaller units, the subsequent refusion into a nanograph domain, and the growth of GQDs [61,62]. Overall, the possibilities of the bottom-up method to utilize biomass derivatives as GQDs precursors have gained much interest nowadays, in order to realize a more sustainable, green, and eco-friendly approach to synthesize GQDs with unique properties and controlled structures to be usable for many applications.

Table 1. Characteristics of top-down and bottom-up methods in the synthesis of GQDs.

	Subgroup	Initial Material	Size (nm)	Quantum Efficiency	Ref.
Top-down	Acid oxidation	Carbon black	15	44.5	[63]
	Hydrothermal	Graphene oxide	5–13	5	[64]
	Solvothermal	Graphene oxide	3–5	1.6	[65]
	Microwave	Graphene oxide	2–7	8	[66]
	Ultrasound waves	Graphene	3–5	-	[54]
Bottom-up	Electrochemical	Graphite	5–10	-	[67]
	Pyrolysis of the precursor	Glucose	1.65–21	-	[68]
	Catalytic opening of the cage	Fullerene 60	2.7–10	15–30	[46]
	Pyrolysis	Hexa benzo chromen	~60	-	[69]

2.2. Plasma Synthesis of GQDs

Plasma synthesis is considered one of the most popular gas-phase methods for the preparation of various GQDs, especially those with covalent bonding [70–72]. For example, QDs of germanium (Ge) and silicon (Si) have been synthesized using a conventional non-thermal plasma. In non-thermal plasma, factors, such as shape, surface area, quantum dot composition and size, can be controlled [73,74]. Plasma synthesis achieves doping, which is a major challenge for QDs [75–77]. GQDs synthesized by plasma usually take the form of powder, which can lead to surface modification. This can lead to excellent dispersion of QDs in water [78] or organic solvents [79] (i.e., colloidal quantum dots).

2.3. Method of Bioactivation

2.3.1. Bioactive Carbon Sources

The development of bioactive materials for biomedical applications, such as inflammation therapy, is desirable if it is compatible with detectable properties and integrates efficient differentiation into biocompatible procedures. It has been possible to fabricate bioactive carbon dots (CD) with a size of about 4 nm, which have low toxicity, interesting safety responses, and unique photophysical properties. Bioactive CDs were prepared by a novel one-step hydrothermal method from aspirin and adenosine [80–83]. Multipurpose CDs are designed and fabricated using a bottom-up synthesis strategy to further manipulate chemical compounds and physical properties by introducing complex bioactive precursors, including nucleic acids, proteins, and small molecules. These bioactive CDs have different pharmacological activity from conventional citric acid-based CDs to expand their potential applications against pathogens and cancer [84,85].

2.3.2. Biomass-Waste Derived GQD

Due to increasing customer demand, energy crisis and environmental degradation, scientists are looking for cost-effective, environmentally friendly, and easy ways to produce new advanced materials from renewable sources. Recently, graphene quantum dots (GQDs) have attracted much attention compared to other investigated materials, such as carbon-based nanomaterials, due to their attractive properties, such as low toxicity, long lifetime, high conductivity, good biocompatibility, and large surface area. Therefore, the properties of biomass waste-derived GQDs have been modified by adding surface inactivating agents and various functional groups through surface processing [31,86]. Kalita et al. investigated the modification of GQDs by amine functionalization to enhance the quantum efficiency of rice grain-derived GQDs. The results showed that the quantum efficiency was improved by 125% after amine functionalization, which was attributed to the superior electron donating ability of amine groups [31,86]. Table 2 shows the synthesis of GQD from different types of biomass waste. Figure 3a,b show GQDs obtained from biowaste and different approaches to convert biowaste into GQDs, with a description of their use as energy sources.

Table 2. Synthesis of GQDs from different types of biomass-waste.

Precursor	Product	Preparation Approach	Size (nm)	Ref.
Rice grains	GQDs	Pyrolysis	2–6.5	[87]
Fenugreek leaf extract	GQDs	Pyrolysis and hydrothermal treatment	3–10	[88]
Wood charcoal	GQDs	Electrochemical oxidation	3–6	[89]
Neem leaves	GQDs, Am-GQDs	Pyrolysis and hydrothermal treatments	5–6	[90]
Coffee grounds	GQDs, PEIGQDs	Hydrothermal treatment	1.88 (GQDs) 2.67 (PEIGQDs)	[91]

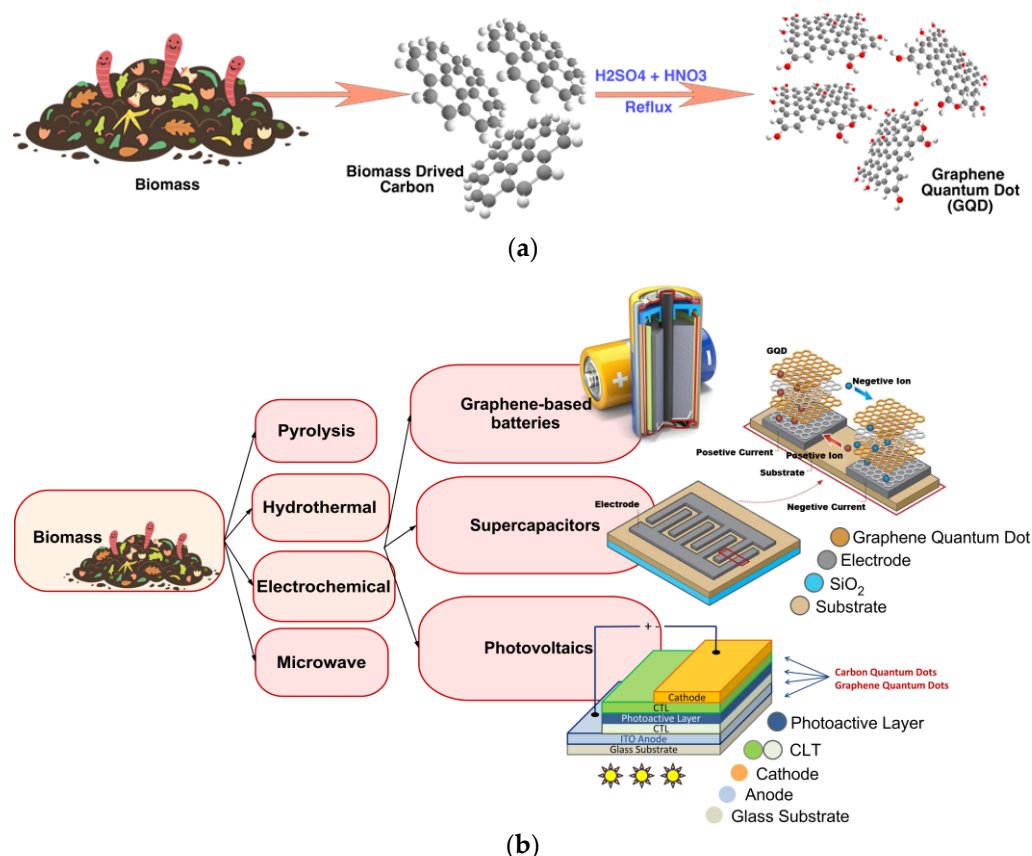


Figure 3. (a) The synthesis of GQD ($C_{57}H_{26}O_{11}$) from different types of biomass-waste; (b) figure illustrates the various approaches used for converting biowaste into GQDs, along with how they can be used as energy sources.

2.3.3. Biologically Active Agents

Bioactive agents are factors that affect a living organ, cell, or tissue. They may be bioactive compounds, vitamins, drugs, phytochemicals, or enzymes. Bioactive agents used in biomedical devices and drugs can be contained in polymers [92]. The loading of bioactive agents in drug delivery systems is carried out by enzymatically reacting polymers and the cleavage of these agents by the target enzymes. The release of the therapeutic cargo occurs through the activation of the bioactive agents [93].

3. SERS GQD

The frequency of the Raman peak of a phonon can be related to the chemical composition, the internal stress or surface state, and the shape and size of the GQD. Applications of Raman spectroscopy include the multiplexed detection of biomarkers from various compounds, controlling the synthesis of GQDs, studying vibrational properties associated

with relaxation mechanisms, and analysing QDs. For example, Raman spectra are associated with different concentrations of alloying constituents for alloyed QDs, and this spectrum is also used to indicate the formation of quantum dots [94,95]. Therefore, the use of surface-enhanced Raman spectroscopy (SERS) is possible when the Raman intensity is undetectable and very low, such as the deposition of nanoparticles on a metal film, such as Ag, Al, or Au; these films have surface plasmon states with very limited electromagnetic fields that support emission and light absorption at the interface between air and metal. SERS also has applications from vibrational spectroscopy or photochemical studies [96] to the single emitter level [97,98], such as the detection of bacteria or impurities, and chemical analysis. Since different fabrication methods and many substrates have been proposed, it can be said that in the search for efficient and cheap metal substrates, SERS is a very active field. Examples are the gold nanoparticles recently obtained by the femtosecond exposure of a gold film [99], the strips of vertical or horizontal gold nanorods [100], the dual pyramidal gold nanoparticles [101], or the growth of silver nanoparticles on Si by the alternative method [100]. Hot spots occur when the key element is the presence of sharp points or dents on the surface of the metal substrate, where plasmonic states can be strongly confined. Hot spots are also crucial for future plasmonic applications in photochemistry or photovoltaics [96]. Some works have applied SERS to QDs made of different materials: SnO₂ [102], Si [103], CdS [104], PbS [105], or CdSe [106–108]. Thus, SERS is used as a promising technique for QD detection; biomarker detection; in situ tracking of nanoparticle surface chemical properties, such as oxidation; and nanoparticle impact detection [26,103,105]. SERS in QDs can be very useful because the material is not only environmentally friendly and compatible with the SERS mechanism but also has a large specific surface area, biocompatibility, and high chemical stability [109], which supports the improvement process of the mechanism for the improved detection of QDs SERS. Although previous work SERS has reported QDs in solid form, compared to QDs in solution-based formats, it may require a complex process to use QDs in solid form for other SERS applications. In addition, solution-based QDs can be synthesized by a top-down approach, such as an electrochemical method that provides the ability to obtain SERS of QDs in solution. This method uses the electric field as a mechanism to support the enhanced SERS detection of QDs in the chemical mechanism (CM) to initiate the contact process of molecules and chemical reactions [110]. A schematic representation of the mechanism of SERS QDs for analyte detection can be found in Figure 4. Graphene and other 2D materials have been developed for use as Raman enhancement substrates. This is due to their unique single sheet of carbon atoms in a 2D honeycomb crystal structure of electrons and phonons with one 2p_z orbital of each sp² hybridized carbon atom constituting a large, delocalized bond, forming an ideal flat surface and strong chemical interaction with many organic molecules [111]. As a SERS platform, graphene thus enables the independent investigation of the chemical enhancement mechanism (CM). Graphene may boost the Raman signals of molecules that have been adsorbed, and these substrates have shown to be promising for the detection of micro- and trace species. This impact was identified for the first time in 2010 by Ling et al. [112]. When graphene is treated with organic solvents, several “emerging bands” form on mechanically exfoliated graphene [113]. These “emerging bands” are scattered among the unidentified organic compounds included in the transparent tape used for graphene exfoliation. Graphene has a Raman amplification effect on trace residues. QDs SERS is useful for both the fundamental investigations of SERS phenomena and several practical applications because of the graphene matrix’s significant benefits, such as homogeneity, repeatability, cleanliness, and low detection limit for aromatherapy dyes. Graphene makes SERS applications of Raman-enhanced substrates more quantitatively controlled.

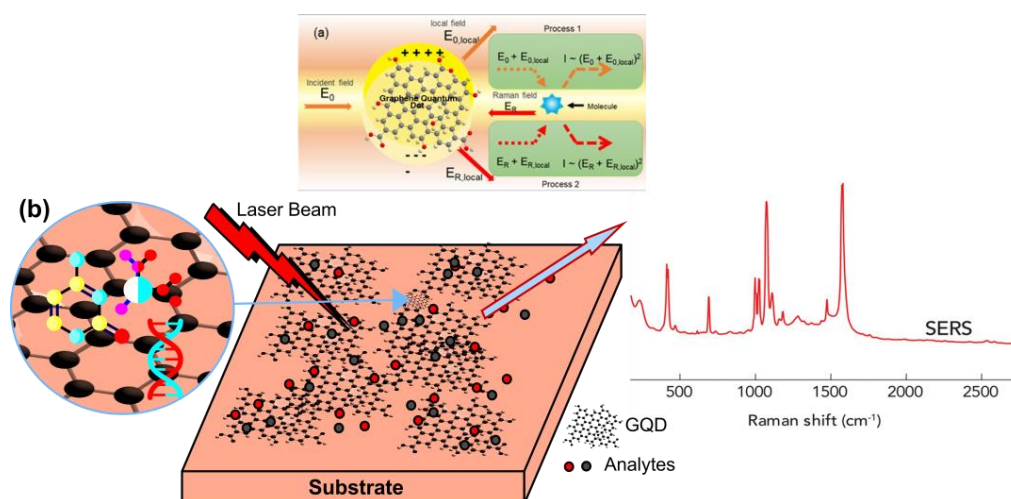


Figure 4. (a) Mechanism of the surface-enhanced Raman scattering (SERS) electromagnetic (EM) effect, electromagnetic SERS enhancement. Reprinted with permission from [114]. Copyright © 2020, American Chemical Society. (b) Schematic illustration of molecules on graphene and a substrate and Raman experiments. Reprinted with permission from [112], Copyright © 2010, American Chemical Society.

4. Detection Mechanisms of SERS

Since the discovery of SERS, several mechanisms have been proposed, but only two are widely accepted today: the electromagnetic theory (EM) and the chemical amplification theory (CE). The EM theory is more dominant because it can amplify the Raman signal up to ten thousand times. While CE amplifies the Raman signal up to 100 times. In the EM model, the laser interacts with the metal surface. As a result of this interaction, dissolved surface plasmons are stimulated, which amplify the field near the surface. In the CE theory, the electron states of the adsorbent change due to chemical adsorption. In the SERS phenomenon, both factors occur simultaneously, which is why the Raman signal can be amplified to such an extent. In general, surface-enhanced Raman spectroscopy is very similar to Raman resonance spectroscopy. The difference being that the resonances present are not exclusively of the intramolecular type. Surface-enhanced Raman spectroscopy or SERS is also a method of Raman spectroscopy that has very high sensitivity in deciphering materials [115–117]. This method has numerous applications in medical science. Since it does not damage natural tissues, it does not require sample preparation and is very rapid. Therefore, this method is used to detect proteins in body fluids. It is also used for diagnosis and treatment of tumours and cancer, the treatment of neurological diseases, the detection of COVID-19, and the detection of coronavirus RNA. This technology for detecting urea and label-free plasma in human serum can be useful in cancer screening. SERS can be used for drugs, forensics, the detection of drugs and explosives, the study of redox processes at the single molecule level, the quantitative analysis of small molecules in human biological fluids, the quantitative detection of biomolecular interactions and more. In a tumour testing, the tumour is grown in vitro. In reality, the test is performed on living tissue (these tests are called in vivo tests). SERS can be used to detect low molecular weight biomolecules (Figure 5) [118–121]. Moreover, the mechanism of SERS detection in the efficiency of GQDs due to surface factorization and heteroatomic doping has been discussed in few studies. Therefore, in the near future, in-depth studies on these topics, which open a new window to developing highly effective improved GQDs SERS, will help scientists and researchers to understand the inflammatory diagnosis of GQDs. Finally, low-cost industrial production is urgently needed to develop and expand these approaches in the near future. To diagnose the inflammation and interior of GQDs and control the macroscopic properties of GQDs, one must be able to produce GQDs by controlling their size as much as possible [122].

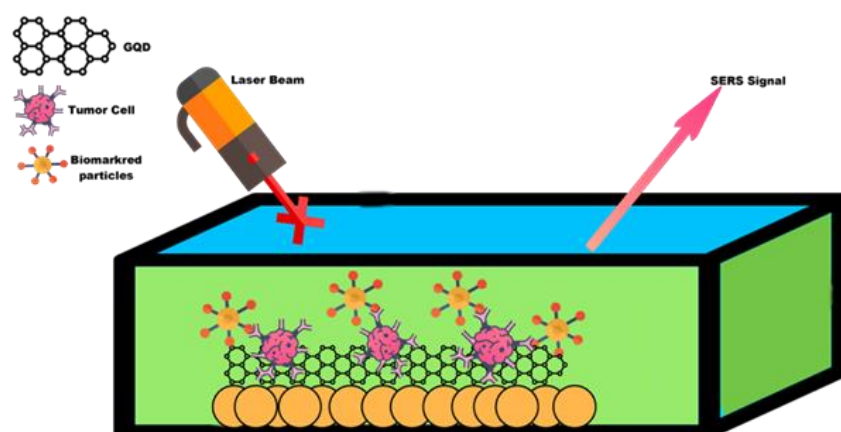


Figure 5. In vivo imaging of SERS-enhanced GQDs for detection of tumours, inflammation and living tissues.

5. Inflammatory Biomarkers

The term biomarker was first used by the National Institutes of Health in the United States in 1980 [123]. Biomarkers are a new method in medicine in which these markers measure specific indicators and examine routine biological processes, pathological processes, or pharmacological responses through therapeutic or health mediators. Specific RNA/DNA gene sequences, antibody determinations, and organic metabolite measurements are also identified [124–126]. For example, blood pressure is a biomarker for stroke risk and glucose levels are a biomarker for patients with diabetes; cholesterol levels are also used to determine cardiovascular disease risk [127]. For the nervous system, muscle, blood, nerve, cerebrospinal fluid, skin, and urine have been used to extract information from the brain in healthy and unhealthy states. These tools and technologies directly measure biological factors (such as blood or CSF) or they work together with brain imaging to measure changes in the composition, function, and structure of the nervous system. Biomarkers are classified according to the sequence of events from “exposure” to “disease”. Biomarker “exposure” is used to predict hazards and to establish a link between external exposures and internal dosimetry. Disease biomarkers are used for the screening, identification, and monitoring of disease progression [128–130]. In addition, these biomarkers can be used to refine drugs to improve therapeutic outcome and health [127]. A good biomarker must be more than 80% specific and have an equally high sensitivity (above 80). The role of biomarkers is not only identification, but they also have the potential to be predictive or play a role in the development of new therapies [131]. Plasma biomarkers are divided into pro-inflammatory biomarkers that include the following subgroups [132]:

5.1. C-Reactive Protein and Cytokines

C-reactive protein (CPR) is a protein involved in host safety and is mainly released by adipose tissue and liver in response to inflammatory stress. On the other hand, its reaction with the crystallisable receptor fragment leads to the production of pre-inflammatory cytokines. According to studies, CRP levels increase in patients with migraines and in women who suffer migraines with aura [132–134]. Cytokines are small proteins that are released by the stimulating neuropeptides involved in migraines. Therefore, their serum levels increase during migraine attacks, for example [132]: Tumour necrosis factor alpha (TNF- α), as a proinflammatory cytokine, plays a key role in the regulation of immune cells; it is also involved in clot formation, cell proliferation, apoptosis, lipid metabolism, and increases in plasma after migraine attacks. Transforming growth factor beta 1 (TGF- β 1), a proinflammatory cytokine, also has several functions. This type of cytokine not only plays an important role in immune system function and blood vessel formation, but also causes motility, apoptosis, cell growth control, and differentiation [132,134,135]. TGF- β 1 levels are increased in migraine patients compared to controls [133], but there is no difference

between levels in aura and without aura. Fatigue and lack of energy during migraines are due to increased TGF- β 1 levels [136]. Figure 6 shows a schematic of C-reactive proteins and cytokines, the functional pathways of CRP. As a result of cytokines, such as IL6 and IL1*, hepatic CRP expression increases significantly. CRP circulates, opsonizing bacteria and apoptotic cells so they can be cleared through the complement system. Immunomodulatory cytokines, such as IL10, may be released by phagocytic cells in response to CRP ligation. Studies have found that plasma CRP deposited onto inflamed tissue breaks down into biologically active monomeric subunits, which can be credited with proinflammatory effects.

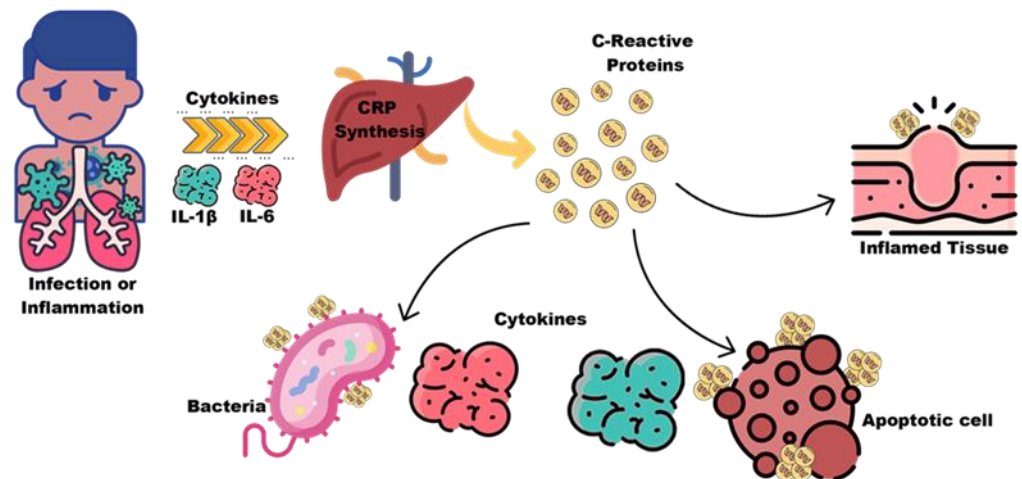


Figure 6. Schematic of C-reactive protein and cytokines the functional pathways of CRP.

5.2. Adiponectin and Lipids

Adiponectin is released from adipose tissue and is an anti-inflammatory cytokine, like IL-10, that inhibits the expression of pre-inflammatory cytokines. It plays an important role in regulating glucose homeostasis and other metabolic processes and is associated with obesity and BMI [132,133]. Research shows that lipids are associated with high cholesterol and migraine. In addition to total cholesterol, there is evidence that people with migraine have further increases in lipid subtypes, such as low-density lipoprotein cholesterol, oxidised LDL-c, triglycerides, and also a decrease in the anti-inflammatory high-density lipoprotein cholesterol [132,137]. Figure 7 shows the main processes by which adiponectin maintains metabolic homeostasis.

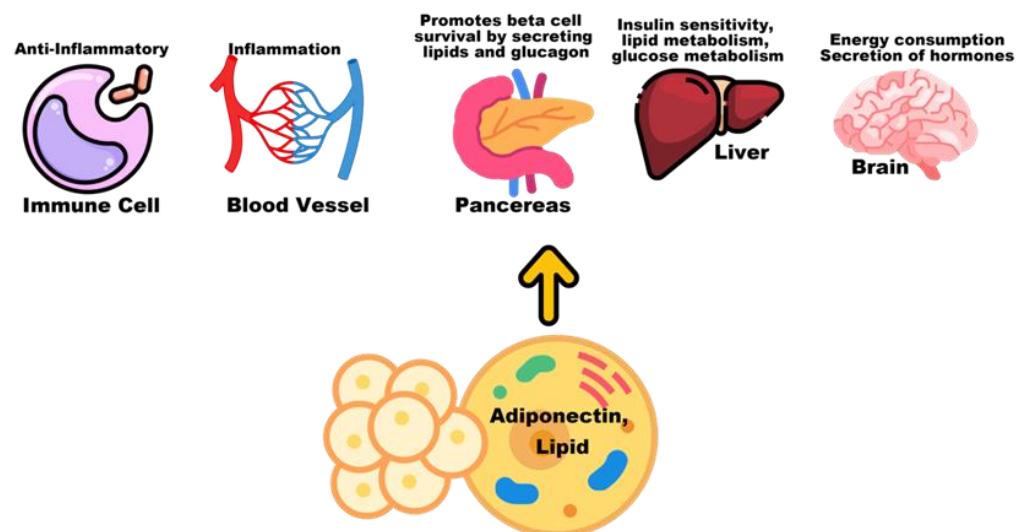


Figure 7. The major processes through which adiponectin maintains metabolic homeostasis.

5.3. Raman Spectrum of the Inflammatory Biomarkers

Recently, biomarker detection based on Raman spectrum technology has been widely and comprehensively developed. Raman spectrum technology has attracted more attention with the rapid development of nanotechnology. Raman spectrum technology plays an important diagnostic role from organelle functionality, inflammation detection, and virus detection to cell activity detection. However, there are still many challenges in the development of Raman spectrum technology [138,139]. Monitoring different types of inflammation in the early stages by *in vitro* diagnosis is vital. For early detection and prognosis of inflammation, biomarkers, such as proteins, miRNAs, DNAs, and other biomolecules, must be evaluated [140,141]. The specificity and sensitivity of the Raman spectrum make it possible to accurately detect related physiological analytes in complex biological fluids. To detect inflammatory biomarkers, the Raman spectrum is linked to relevant detection molecules (such as antibodies and aptamers) to allow specific targets to be measured with Raman signals [142,143].

6. Detection of Inflammatory

The immune system is involved in the development of a variety of diseases [144–146]. The regulation of immune responses by direct tissue imaging in diseases, such as atherosclerosis [147], rheumatoid arthritis [148], malaria [149], and stroke [150], is due to the increasing interest in understanding the molecular and cellular interactions of the pathway. A number of intravital microscopy techniques have been used to study these interactions. For example, the two-photon fluorescence microscope (TPM) has become the method of choice for stimulating fluorophores deep within tissues due to its unique ability to produce light in the near-infrared range. However, successful imaging is limited to depths of a few hundred micrometres [151]. In addition, fluorescence imaging produces a broad emission spectrum [152] that often leads to photobleaching [153], as this imaging generally suffers from poor discrimination between specific fluorophores and background autofluorescence beyond a small optical window [154]. One way to enhance the Raman signal is to use the SERS method. This method involves vibrational spectroscopy in which molecules are adsorbed onto a metal surface with a nano-sized surface area. SERS-activated GQDs were encoded with a unique Raman signal that was monitored under a wide range of excitations and conditions. GQDs containing active Raman molecules were conjugated with specific monoclonal antibodies against intercellular adhesion molecule 1 (ICAM-1) to detect early-stage inflammation. The non-invasive measurement of ICAM-1 expression by SERS is possible *in vivo* with double the sensitivity of double photon fluorescence [155]. Therefore, a new approach for the diagnosis of inflammation *in vivo* using GQDs SERS was considered. Using a metal surface to enhance Raman scattering from molecules located near or attached to the surface results in vibrational spectroscopy called SERS. A wide range of different surfaces and metals can be used to achieve this goal. GQDs, however, offer a great format. By binding molecules with a unique and strong Raman spectrum, called Raman reporters, to GQDs and encapsulating them in a silicon-containing shell, GQDs with improved SERS are produced. The Raman reporter molecules are protected by a silica shell that acts as a coating and gives the GQD a unique and strong SERS signal [156,157]. *In vivo* imaging of SERS-enriched GQDs has also been used to monitor inflammation and reuse. Although this is not a disease process, it is still important as any changes may indicate infection and non-hidden disease states Figure 8 [155].

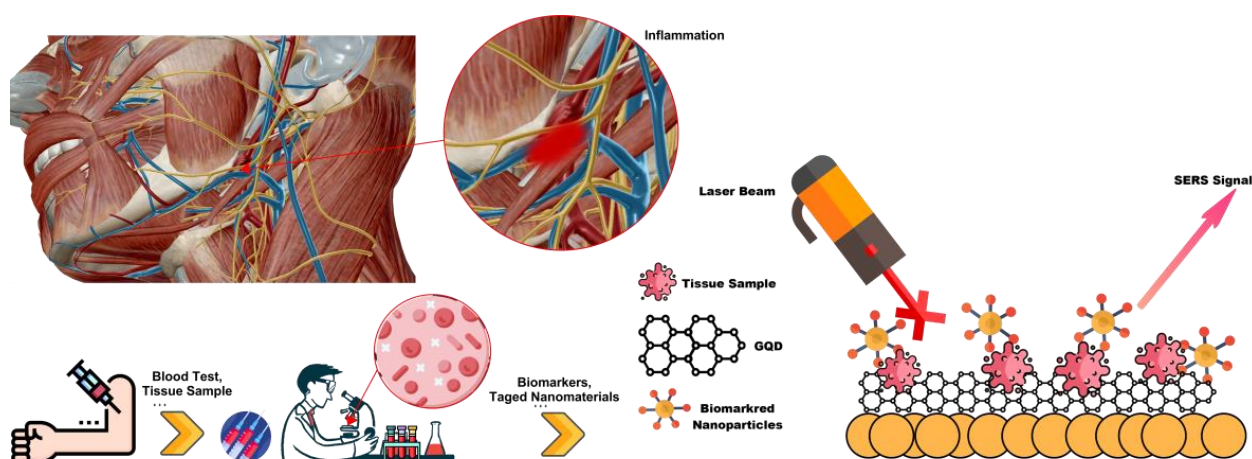


Figure 8. Detection of inflammatory by SERS-enhanced GQDs.

7. Perspectives

The multiple applications of Raman and the significant improvement of GQDs SERS for the diagnosis of inflammatory diseases are direct consequences of the numerous advantages they offer. Unlike their fluorescent counterparts, they produce specific, sharp molecular spectra that give these techniques immediate and easy access to multiple ways of diagnosing disease. In addition, there is the possibility of combined Raman and SERS imaging of tissues and cells, so that biochemical information and features of the inflammatory process can be obtained simultaneously as active SERS nanotags are formed. To improve GQDs SERS and remain at the forefront of inflammatory disease diagnosis, further studies in physiological representative media, clinical samples, and *in vivo* are required. Once these programmes have fully demonstrated their reproducibility, sensitivity, robustness, repeatability and selectivity *in vivo*, the laboratory will be transferred to a clinical setting. Once these applications have fully demonstrated their techniques, sensitivity, and reliability they will be strong contenders that will revolutionise our ability to diagnose inflammatory diseases. Ultimately, the hope is that the use of GQDs, which SERS enhance for the *in vivo* diagnosis of inflammation, will be part of a growing toolkit for next-generation non-invasive imaging and *in vivo* diagnosis.

8. Conclusions

This review summarises recent advances in the diagnosis of inflammation using graphene quantum dot SERS. Three subtopics are described, including the method of GQD synthesis, the method of bioactivation, inflammatory biomarkers, the plasma synthesis of GQDs and SERS GQD, and the detection mechanisms of SERS and the detection of inflammation. There are key points in the development of SERS GQD and its biomedical applications, as the rapid evolution of SERS GQD from biological to biomedical applications has been remarkable over the past decades. Significant progress has been made in improving diagnostic sensitivity and multiplexity. Recent advances have led to SERS GQD being used to diagnose inflammation in necrotic tissue and damaged cells, which will be of great importance for use in medical facilities. In short, SERS GQD has the advantageous properties of unprecedented multiplexing capability, perfect signal specificity and high sensitivity. Therefore, there are driving forces to exploit these properties for important applications. However, there are still some steps to be taken when using SERS GQD for clinical applications.

Author Contributions: S.M.M. and A.G. developed the idea and structure of the review article. V.R., S.A.H. and M.Y.K. wrote the manuscript, collecting the materials from databases. N.O., D.K. and A.G. revised and improved the manuscript. A.G. and W.-H.C. supervised the manuscript. All authors have read and agreed to the published version of the manuscript.

Funding: This work is sponsored by the Ministry of Science and Technology, Taiwan (grant number: MOST 110-2628-E-011-003, MOST 109-2923-E-011-003-MY, MOST 111-NU-E-011-001-NU).

Institutional Review Board Statement: Not applicable.

Informed Consent Statement: Not applicable.

Data Availability Statement: All data generated or analysed during this study are included in the published article.

Conflicts of Interest: The authors declare no conflict of interest.

References

1. Khan, S.; Nisar, M.; Rehman, W.; Khan, R.; Nasir, F. Anti-inflammatory study on crude methanol extract and different fractions of *Eremostachys laciniata*. *Pharm. Biol.* **2010**, *48*, 1115–1118. [[CrossRef](#)] [[PubMed](#)]
2. Stewart, F.; Akleyev, A.; Hauer-Jensen, M.; Hendry, J.; Kleiman, N.; Macvittie, T.; Aleman, B.; Edgar, A.; Mabuchi, K.; Muirhead, C. ICRP publication 118: ICRP statement on tissue reactions and early and late effects of radiation in normal tissues and organs—threshold doses for tissue reactions in a radiation protection context. *Ann. ICRP* **2012**, *41*, 1–322. [[CrossRef](#)] [[PubMed](#)]
3. Kalashgarani, M.Y.; Babapoor, A. Application of nano-antibiotics in the diagnosis and treatment of infectious diseases. *Adv. Appl. NanoBio-Technol.* **2022**, *3*, 22–35.
4. Mousavi, S.M.; Hashemi, S.A.; Amani, A.M.; Saed, H.; Jahandideh, S.; Mojoudi, F. Polyethylene terephthalate/acryl butadiene styrene copolymer incorporated with oak shell, potassium sorbate and egg shell nanoparticles for food packaging applications: Control of bacteria growth, physical and mechanical properties. *Polym. Renew. Resour.* **2017**, *8*, 177–196. [[CrossRef](#)]
5. Fairweather, D. Atherosclerosis and Inflammatory Heart Disease. In *Immunotoxicity, Immune Dysfunction, and Chronic Disease*; Springer: Berlin/Heidelberg, Germany, 2012; pp. 271–289.
6. Pascoal, A.; Estevinho, M.M.; Choupina, A.; Sousa-Pimenta, M.; Estevinho, L.M. An overview of the bioactive compounds, therapeutic properties and toxic effects of apitoxin. *Food Chem. Toxicol.* **2019**, *134*, 1–11. [[CrossRef](#)] [[PubMed](#)]
7. Alipour, A.; Kalashgarani, M.Y. Nano Protein and Peptides for Drug Delivery and Anticancer Agents. *Adv. Appl. NanoBio-Technol.* **2022**, *3*, 60–64.
8. Mousavi, S.M.; Hashemi, S.A.; Esmaeili, H.; Amani, A.M.; Mojoudi, F. Synthesis of Fe₃O₄ nanoparticles modified by oak shell for treatment of wastewater containing Ni (II). *Acta Chim. Slov.* **2018**, *65*, 750–756. [[CrossRef](#)] [[PubMed](#)]
9. Mc-Namara, D.; Mayeux, P. Nonopioid analgesics and anti-inflammatory drugs. In *Principles of Pharmacology: Basic Concepts and Clinical Applications*, 3rd ed.; Int. Thomson Publ. Co., Chapman Hall: Pacific Grove, CA, USA, 1995; pp. 1160–1178.
10. Mousavi, S.; Hashemi, S.; Gholami, A.; Kalashgarani, M.; Vijayakameswara Rao, N.; Omidifar, N.; Hsiao, W.; Lai, C.; Chiang, W. Plasma-Enabled Smart Nano Exosome Platform as Emerging Immunopathogenesis for Clinical Viral Infection. *Pharmaceutics* **2022**, *14*, 1054. [[CrossRef](#)]
11. Xie, R.; Wang, Z.; Zhou, W.; Liu, Y.; Fan, L.; Li, Y.; Li, X. Graphene quantum dots as smart probes for biosensing. *Anal. Methods* **2016**, *8*, 4001–4016. [[CrossRef](#)]
12. Kazemi, K.; Ghahramani, Y.; Kalashgarani, M.Y. Nano biofilms: An emerging biotechnology applications. *Adv. Appl. NanoBio-Technol.* **2022**, *3*, 8–15.
13. Farshbaf, M.; Davaran, S.; Rahimi, F.; Annabi, N.; Salehi, R.; Akbarzadeh, A. Carbon quantum dots: Recent progresses on synthesis, surface modification and applications. *Artif. Cells Nanomed. Biotechnol.* **2018**, *46*, 1331–1348. [[CrossRef](#)]
14. Mousavi, S.M.; Hashemi, S.A.; Kalashgarani, M.Y.; Gholami, A.; Omidifar, N.; Babapoor, A.; Vijayakameswara Rao, N.; Chiang, W.-H. Recent Advances in Plasma-Engineered Polymers for Biomarker-Based Viral Detection and Highly Multiplexed Analysis. *Biosensors* **2022**, *12*, 286. [[CrossRef](#)] [[PubMed](#)]
15. Lee, B.-C.; Lee, J.Y.; Kim, J.; Yoo, J.M.; Kang, I.; Kim, J.-J.; Shin, N.; Kim, D.J.; Choi, S.W.; Kim, D. Graphene quantum dots as anti-inflammatory therapy for colitis. *Sci. Adv.* **2020**, *6*, eaaz2630. [[CrossRef](#)]
16. Mousavi, S.; Arjmand, O.; Hashemi, S.; Banaei, N. Modification of the epoxy resin mechanical and thermal properties with silicon acrylate and montmorillonite nanoparticles. *Polym. Renew. Resour.* **2016**, *7*, 101–113. [[CrossRef](#)]
17. Qian, X.-M.; Nie, S.M. Single-molecule and single-nanoparticle SERS: From fundamental mechanisms to biomedical applications. *Chem. Soc. Rev.* **2008**, *37*, 912–920. [[CrossRef](#)] [[PubMed](#)]
18. Gubala, V.; Harris, L.F.; Ricco, A.J.; Tan, M.X.; Williams, D.E. Point of care diagnostics: Status and future. *Anal. Chem.* **2012**, *84*, 487–515. [[CrossRef](#)]
19. Bonaccorso, F.; Colombo, L.; Yu, G.; Stoller, M.; Tozzini, V.; Ferrari, A.C.; Ruoff, R.S.; Pellegrini, V. Graphene, related two-dimensional crystals, and hybrid systems for energy conversion and storage. *Science* **2015**, *347*, 1246501. [[CrossRef](#)]
20. Tian, L.; Tadepalli, S.; Fei, M.; Morrissey, J.J.; Kharasch, E.D.; Singamaneni, S. Off-resonant gold superstructures as ultrabright minimally invasive surface-enhanced Raman scattering (SERS) probes. *Chem. Mater.* **2015**, *27*, 5678–5684. [[CrossRef](#)]
21. Ma, Y.; Promthaveepong, K.; Li, N. Chemical sensing on a single SERS particle. *ACS Sens.* **2017**, *2*, 135–139. [[CrossRef](#)]
22. Huang, C.W.; Hao, Y.W.; Nyagilo, J.; Dave, D.P.; Xu, L.F.; Sun, X.K. Porous hollow gold nanoparticles for cancer SERS imaging. In *Journal of Nano Research*; Trans Tech Publications Ltd.: Bäch SZ, Switzerland, 2010; pp. 137–148.

23. Pinkhasova, P.; Puccio, B.; Chou, T.; Sukhishvili, S.; Du, H. Noble metal nanostructure both as a SERS nanotag and an analyte probe. *Chem. Commun.* **2012**, *48*, 9750–9752. [[CrossRef](#)]
24. Emami-Meibodi, M.; Parsaeian, M.; Amraei, R.; Banaei, M.; Anvari, F.; Tahami, S.; Vakhshoor, B.; Mehdizadeh, A.; Nejad, N.F.; Shirmardi, S. An experimental investigation of wastewater treatment using electron beam irradiation. *Radiat. Phys. Chem.* **2016**, *125*, 82–87. [[CrossRef](#)]
25. Amani, A.M.; Hashemi, S.A.; Mousavi, S.M.; Abrishamifar, S.M.; Vojood, A. Electric field induced alignment of carbon nanotubes: Methodology and outcomes. In *Carbon Nanotubes-Recent Progress*; IntechOpen: London, UK, 2017.
26. Mousavi, S.M.; Hashemi, S.A.; Jahandideh, S.; Baseri, S.; Zarei, M.; Azadi, S. Modification of phenol novolac epoxy resin and unsaturated polyester using sasobit and silica nanoparticles. *Polym. Renew. Resour.* **2017**, *8*, 117–132. [[CrossRef](#)]
27. Xu, W.; Ling, X.; Xiao, J.; Dresselhaus, M.S.; Kong, J.; Xu, H.; Liu, Z.; Zhang, J. Surface enhanced Raman spectroscopy on a flat graphene surface. *Proc. Natl. Acad. Sci. USA* **2012**, *109*, 9281–9286. [[CrossRef](#)]
28. Mousavi, S.M.; Zarei, M.; Hashemi, S.A.; Ramakrishna, S.; Chiang, W.-H.; Lai, C.W.; Gholami, A.; Omidifar, N.; Shokripour, M. Asymmetric membranes: A potential scaffold for wound healing applications. *Symmetry* **2020**, *12*, 1100. [[CrossRef](#)]
29. Cheng, H.; Zhao, Y.; Fan, Y.; Xie, X.; Qu, L.; Shi, G. Graphene-quantum-dot assembled nanotubes: A new platform for efficient Raman enhancement. *ACS Nano* **2012**, *6*, 2237–2244. [[CrossRef](#)]
30. Mehrabani, J.; Mousavi, S.; Noaparast, M. Evaluation of the replacement of NaCN with Acidithiobacillus ferrooxidans in the flotation of high-pyrite, low-grade lead–zinc ore. *Sep. Purif. Technol.* **2011**, *80*, 202–208. [[CrossRef](#)]
31. Hashemi, S.A.; Mousavi, S.M. Effect of bubble based degradation on the physical properties of Single Wall Carbon Nanotube/Epoxy Resin composite and new approach in bubbles reduction. *Compos. Part A Appl. Sci. Manuf.* **2016**, *90*, 457–469. [[CrossRef](#)]
32. Zheng, X.T.; Ananthanarayanan, A.; Luo, K.Q.; Chen, P. Glowing graphene quantum dots and carbon dots: Properties, syntheses, and biological applications. *Small* **2015**, *11*, 1620–1636. [[CrossRef](#)]
33. Xu, X.; Ray, R.; Gu, Y.; Ploehn, H.J.; Gearheart, L.; Raker, K.; Scrivens, W.A. Electrophoretic analysis and purification of fluorescent single-walled carbon nanotube fragments. *J. Am. Chem. Soc.* **2004**, *126*, 12736–12737. [[CrossRef](#)]
34. Ju, S.-Y.; Kopcha, W.P.; Papadimitrakopoulos, F. Brightly fluorescent single-walled carbon nanotubes via an oxygen-excluding surfactant organization. *Science* **2009**, *323*, 1319–1323. [[CrossRef](#)]
35. Guo, X.; Wang, C.-F.; Yu, Z.-Y.; Chen, L.; Chen, S. Facile access to versatile fluorescent carbon dots toward light-emitting diodes. *Chem. Commun.* **2012**, *48*, 2692–2694. [[CrossRef](#)]
36. Mousavi, S.M.; Hashemi, S.A.; Zarei, M.; Bahrani, S.; Savardashtaki, A.; Esmaili, H.; Lai, C.W.; Mazraedoost, S.; Abassi, M.; Ramavandi, B. Data on cytotoxic and antibacterial activity of synthesized Fe₃O₄ nanoparticles using Malva sylvestris. *Data Brief* **2020**, *28*, 104929. [[CrossRef](#)]
37. Michalet, X.; Pinaud, F.F.; Bentolila, L.A.; Tsay, J.M.; Doose, S.; Li, J.J.; Sundaresan, G.; Wu, A.; Gambhir, S.; Weiss, S. Quantum dots for live cells, in vivo imaging, and diagnostics. *Science* **2005**, *307*, 538–544. [[CrossRef](#)]
38. Mousavi, S.; Esmaili, H.; Arjmand, O.; Karimi, S.; Hashemi, S. Biodegradation study of nanocomposites of phenol novolac epoxy/unsaturated polyester resin/egg shell nanoparticles using natural polymers. *J. Mater.* **2015**, *2015*, 131957. [[CrossRef](#)]
39. Yu, S.-J.; Kang, M.-W.; Chang, H.-C.; Chen, K.-M.; Yu, Y.-C. Bright fluorescent nanodiamonds: No photobleaching and low cytotoxicity. *J. Am. Chem. Soc.* **2005**, *127*, 17604–17605. [[CrossRef](#)]
40. Baker, S.N.; Baker, G.A. Luminescent carbon nanodots: Emergent nanolights. *Angew. Chem. Int. Ed.* **2010**, *49*, 6726–6744. [[CrossRef](#)]
41. Loh, K.P.; Bao, Q.; Eda, G.; Chhowalla, M. Graphene oxide as a chemically tunable platform for optical applications. *Nat. Chem.* **2010**, *2*, 1015–1024. [[CrossRef](#)]
42. Mousavi, S.; Aghili, A.; Hashemi, S.; Goudarzian, N.; Bakhoda, Z.; Baseri, S. Improved morphology and properties of nanocomposites, linear low density polyethylene, ethylene-co-vinyl acetate and nano clay particles by electron beam. *Polym. Renew. Resour.* **2016**, *7*, 135–153. [[CrossRef](#)]
43. Wang, C.-F.; Sun, X.-Y.; Su, M.; Wang, Y.-P.; Lv, Y.-K. Electrochemical biosensors based on antibody, nucleic acid and enzyme functionalized graphene for the detection of disease-related biomolecules. *Analyst* **2020**, *145*, 1550–1562. [[CrossRef](#)]
44. Lin, L.; Rong, M.; Luo, F.; Chen, D.; Wang, Y.; Chen, X. Luminescent graphene quantum dots as new fluorescent materials for environmental and biological applications. *TrAC Trends Anal. Chem.* **2014**, *54*, 83–102. [[CrossRef](#)]
45. Peng, J.; Gao, W.; Gupta, B.K.; Liu, Z.; Romero-Aburto, R.; Ge, L.; Song, L.; Alemany, L.B.; Zhan, X.; Gao, G. Graphene quantum dots derived from carbon fibers. *Nano Lett.* **2012**, *12*, 844–849. [[CrossRef](#)]
46. Lu, J.; Yeo, P.S.E.; Gan, C.K.; Wu, P.; Loh, K.P. Transforming C60 molecules into graphene quantum dots. *Nat. Nanotechnol.* **2011**, *6*, 247–252. [[CrossRef](#)]
47. Sreeprasad, T.; Rodriguez, A.A.; Colston, J.; Graham, A.; Shishkin, E.; Pallem, V.; Berry, V. Electron-tunneling modulation in percolating network of graphene quantum dots: Fabrication, phenomenological understanding, and humidity/pressure sensing applications. *Nano Lett.* **2013**, *13*, 1757–1763. [[CrossRef](#)]
48. Ye, R.; Xiang, C.; Lin, J.; Peng, Z.; Huang, K.; Yan, Z.; Cook, N.P.; Samuel, E.L.; Hwang, C.-C.; Ruan, G. Coal as an abundant source of graphene quantum dots. *Nat. Commun.* **2013**, *4*, 2943. [[CrossRef](#)]
49. Yan, Y.; Chen, J.; Li, N.; Tian, J.; Li, K.; Jiang, J.; Liu, J.; Tian, Q.; Chen, P. Systematic bandgap engineering of graphene quantum dots and applications for photocatalytic water splitting and CO₂ reduction. *ACS Nano* **2018**, *12*, 3523–3532. [[CrossRef](#)]

50. Shin, Y.; Park, J.; Hyun, D.; Yang, J.; Lee, J.-H.; Kim, J.-H.; Lee, H. Acid-free and oxone oxidant-assisted solvothermal synthesis of graphene quantum dots using various natural carbon materials as resources. *Nanoscale* **2015**, *7*, 5633–5637. [[CrossRef](#)]
51. Zhang, Y.; Li, K.; Ren, S.; Dang, Y.; Liu, G.; Zhang, R.; Zhang, K.; Long, X.; Jia, K. Coal-derived graphene quantum dots produced by ultrasonic physical tailoring and their capacity for Cu (II) detection. *ACS Sustain. Chem. Eng.* **2019**, *7*, 9793–9799. [[CrossRef](#)]
52. Bacon, M.; Bradley, S.J.; Nann, T. Graphene quantum dots. *Part. Part. Syst. Charact.* **2014**, *31*, 415–428. [[CrossRef](#)]
53. Shen, J.; Zhu, Y.; Chen, C.; Yang, X.; Li, C. Facile preparation and upconversion luminescence of graphene quantum dots. *Chem. Commun.* **2011**, *47*, 2580–2582. [[CrossRef](#)]
54. Li, Y.; Hu, Y.; Zhao, Y.; Shi, G.; Deng, L.; Hou, Y.; Qu, L. An electrochemical avenue to green-luminescent graphene quantum dots as potential electron-acceptors for photovoltaics. *Adv. Mater.* **2011**, *23*, 776–780. [[CrossRef](#)]
55. Lee, E.; Ryu, J.; Jang, J. Fabrication of graphene quantum dots via size-selective precipitation and their application in upconversion-based DSSCs. *Chem. Commun.* **2013**, *49*, 9995–9997. [[CrossRef](#)]
56. Dong, Y.; Shao, J.; Chen, C.; Li, H.; Wang, R.; Chi, Y.; Lin, X.; Chen, G. Blue luminescent graphene quantum dots and graphene oxide prepared by tuning the carbonization degree of citric acid. *Carbon* **2012**, *50*, 4738–4743. [[CrossRef](#)]
57. Wu, Z.L.; Gao, M.X.; Wang, T.T.; Wan, X.Y.; Zheng, L.L.; Huang, C.Z. A general quantitative pH sensor developed with dicyandiamide N-doped high quantum yield graphene quantum dots. *Nanoscale* **2014**, *6*, 3868–3874. [[CrossRef](#)]
58. Kumar, S.; Aziz, S.T.; Girshevitz, O.; Nessim, G.D. One-step synthesis of N-doped graphene quantum dots from chitosan as a sole precursor using chemical vapor deposition. *J. Phys. Chem. C* **2018**, *122*, 2343–2349. [[CrossRef](#)]
59. Kurniawan, D.; Chiang, W.-H. Microplasma-enabled colloidal nitrogen-doped graphene quantum dots for broad-range fluorescent pH sensors. *Carbon* **2020**, *167*, 675–684. [[CrossRef](#)]
60. Kurniawan, D.; Anjali, B.A.; Setiawan, O.; Ostrikov, K.K.; Chung, Y.G.; Chiang, W.-H. Microplasma Band Structure Engineering in Graphene Quantum Dots for Sensitive and Wide-Range pH Sensing. *ACS Appl. Mater. Interfaces* **2021**, *14*, 1670–1683. [[CrossRef](#)]
61. Ding, Z.; Li, F.; Wen, J.; Wang, X.; Sun, R. Gram-scale synthesis of single-crystalline graphene quantum dots derived from lignin biomass. *Green Chem.* **2018**, *20*, 1383–1390. [[CrossRef](#)]
62. Kurniawan, D.; Weng, R.-J.; Setiawan, O.; Ostrikov, K.K.; Chiang, W.-H. Microplasma nanoengineering of emission-tunable colloidal nitrogen-doped graphene quantum dots as smart environmental-responsive nanosensors and nanothermometers. *Carbon* **2021**, *185*, 501–513. [[CrossRef](#)]
63. Dong, Y.; Chen, C.; Zheng, X.; Gao, L.; Cui, Z.; Yang, H.; Guo, C.; Chi, Y.; Li, C.M. One-step and high yield simultaneous preparation of single- and multi-layer graphene quantum dots from CX-72 carbon black. *J. Mater. Chem.* **2012**, *22*, 8764–8766. [[CrossRef](#)]
64. Pan, D.; Guo, L.; Zhang, J.; Xi, C.; Xue, Q.; Huang, H.; Li, J.; Zhang, Z.; Yu, W.; Chen, Z. Cutting sp² clusters in graphene sheets into colloidal graphene quantum dots with strong green fluorescence. *J. Mater. Chem.* **2012**, *22*, 3314–3318. [[CrossRef](#)]
65. Li, L.L.; Ji, J.; Fei, R.; Wang, C.Z.; Lu, Q.; Zhang, J.R.; Jiang, L.P.; Zhu, J.J. A facile microwave avenue to electrochemiluminescent two-color graphene quantum dots. *Adv. Funct. Mater.* **2012**, *22*, 2971–2979. [[CrossRef](#)]
66. Chen, S.; Liu, J.-W.; Chen, M.-L.; Chen, X.-W.; Wang, J.-H. Unusual emission transformation of graphene quantum dots induced by self-assembled aggregation. *Chem. Commun.* **2012**, *48*, 7637–7639. [[CrossRef](#)]
67. Shinde, D.B.; Pillai, V.K. Electrochemical preparation of luminescent graphene quantum dots from multiwalled carbon nanotubes. *Chem. – A Eur. J.* **2012**, *18*, 12522–12528. [[CrossRef](#)]
68. Tang, L.; Ji, R.; Cao, X.; Lin, J.; Jiang, H.; Li, X.; Teng, K.S.; Luk, C.M.; Zeng, S.; Hao, J. Deep ultraviolet photoluminescence of water-soluble self-passivated graphene quantum dots. *ACS Nano* **2012**, *6*, 5102–5110. [[CrossRef](#)]
69. Liu, R.; Wu, D.; Feng, X.; Müllen, K. Bottom-up fabrication of photoluminescent graphene quantum dots with uniform morphology. *J. Am. Chem. Soc.* **2011**, *133*, 15221–15223. [[CrossRef](#)]
70. Mangolini, L.; Thimsen, E.; Kortshagen, U. High-yield plasma synthesis of luminescent silicon nanocrystals. *Nano Lett.* **2005**, *5*, 655–659. [[CrossRef](#)]
71. Knipping, J.; Wiggers, H.; Rellinghaus, B.; Roth, P.; Konjhdzic, D.; Meier, C. Synthesis of high purity silicon nanoparticles in a low pressure microwave reactor. *J. Nanosci. Nanotechnol.* **2004**, *4*, 1039–1044. [[CrossRef](#)]
72. Sankaran, R.M.; Holunga, D.; Flagan, R.C.; Giapis, K.P. Synthesis of blue luminescent Si nanoparticles using atmospheric-pressure microdischarges. *Nano Lett.* **2005**, *5*, 537–541. [[CrossRef](#)]
73. Kortshagen, U. Nonthermal plasma synthesis of semiconductor nanocrystals. *J. Phys. D Appl. Phys.* **2009**, *42*, 113001. [[CrossRef](#)]
74. Pi, X.; Kortshagen, U. Nonthermal plasma synthesized freestanding silicon–germanium alloy nanocrystals. *Nanotechnology* **2009**, *20*, 295602. [[CrossRef](#)]
75. Pi, X.; Gresback, R.; Liptak, R.; Campbell, S.; Kortshagen, U. Doping efficiency, dopant location, and oxidation of Si nanocrystals. *Appl. Phys. Lett.* **2008**, *92*, 123102. [[CrossRef](#)]
76. Ni, Z.; Pi, X.; Ali, M.; Zhou, S.; Nozaki, T.; Yang, D. Freestanding doped silicon nanocrystals synthesized by plasma. *J. Phys. D Appl. Phys.* **2015**, *48*, 314006. [[CrossRef](#)]
77. Pereira, R.; Almeida, A. Doped semiconductor nanoparticles synthesized in gas-phase plasmas. *J. Phys. D Appl. Phys.* **2015**, *48*, 314005. [[CrossRef](#)]
78. Pi, X.; Yu, T.; Yang, D. Water-Dispersible Silicon-Quantum-Dot-Containing Micelles Self-Assembled from an Amphiphilic Polymer. *Part. Part. Syst. Charact.* **2014**, *31*, 751–756. [[CrossRef](#)]
79. Mangolini, L.; Kortshagen, U. Plasma-assisted synthesis of silicon nanocrystal inks. *Adv. Mater.* **2007**, *19*, 2513–2519. [[CrossRef](#)]

80. Mousavi, S.M.; Hashemi, S.A.; Kalashgrani, M.Y.; Omidifar, N.; Bahrani, S.; Vijayakameswara Rao, N.; Babapoor, A.; Gholami, A.; Chiang, W.-H. Bioactive Graphene Quantum Dots Based Polymer Composite for Biomedical Applications. *Polymers* **2022**, *14*, 617. [[CrossRef](#)] [[PubMed](#)]
81. Pignatello, R. *Biomaterials Science and Engineering*; BoD—Books on Demand: Norderstedt, Germany, 2011.
82. Horst, F.H.; da Silva Rodrigues, C.V.; Carvalho, P.H.P.R.; Leite, A.M.; Azevedo, R.B.; Neto, B.A.; Corrêa, J.R.; Garcia, M.P.; Alotaibi, S.; Henini, M. From cow manure to bioactive carbon dots: A light-up probe for bioimaging investigations, glucose detection and potential immunotherapy agent for melanoma skin cancer. *RSC Adv.* **2021**, *11*, 6346–6352. [[CrossRef](#)] [[PubMed](#)]
83. Mousavi, S.M.; Hashemi, S.A.; Ramakrishna, S.; Esmaeili, H.; Bahrani, S.; Koosha, M.; Babapoor, A. Green synthesis of supermagnetic Fe₃O₄–MgO nanoparticles via Nutmeg essential oil toward superior anti-bacterial and anti-fungal performance. *J. Drug Deliv. Sci. Technol.* **2019**, *54*, 101352. [[CrossRef](#)]
84. Han, Y.; Zhang, F.; Zhang, J.; Shao, D.; Wang, Y.; Li, S.; Lv, S.; Chi, G.; Zhang, M.; Chen, L. Bioactive carbon dots direct the osteogenic differentiation of human bone marrow mesenchymal stem cells. *Colloids Surf. B Biointerfaces* **2019**, *179*, 1–8. [[CrossRef](#)]
85. Seyed, M.M. Unsaturated polyester resins modified with cresol novolac epoxy and silica nanoparticles: Processing and mechanical properties. *Int. J. Chem. Pet. Sci. (IJCPS)* **2016**, *5*, 13–26.
86. Abbas, A.; Mariana, L.T.; Phan, A.N. Biomass-waste derived graphene quantum dots and their applications. *Carbon* **2018**, *140*, 77–99. [[CrossRef](#)]
87. Kalita, H.; Mohapatra, J.; Pradhan, L.; Mitra, A.; Bahadur, D.; Aslam, M. Efficient synthesis of rice based graphene quantum dots and their fluorescent properties. *RSC Adv.* **2016**, *6*, 23518–23524. [[CrossRef](#)]
88. Roy, P.; Periasamy, A.P.; Chuang, C.; Liou, Y.-R.; Chen, Y.-F.; Joly, J.; Liang, C.-T.; Chang, H.-T. Plant leaf-derived graphene quantum dots and applications for white LEDs. *New J. Chem.* **2014**, *38*, 4946–4951. [[CrossRef](#)]
89. Nirala, N.R.; Khandelwal, G.; Kumar, B.; Prakash, R.; Kumar, V. One step electro-oxidative preparation of graphene quantum dots from wood charcoal as a peroxidase mimetic. *Talanta* **2017**, *173*, 36–43. [[CrossRef](#)]
90. Suryawanshi, A.; Biswal, M.; Mhamane, D.; Gokhale, R.; Patil, S.; Guin, D.; Ogale, S. Large scale synthesis of graphene quantum dots (GQDs) from waste biomass and their use as an efficient and selective photoluminescence on–off–on probe for Ag⁺ ions. *Nanoscale* **2014**, *6*, 11664–11670. [[CrossRef](#)]
91. Wang, L.; Li, W.; Wu, B.; Li, Z.; Wang, S.; Liu, Y.; Pan, D.; Wu, M. Facile synthesis of fluorescent graphene quantum dots from coffee grounds for bioimaging and sensing. *Chem. Eng. J.* **2016**, *300*, 75–82. [[CrossRef](#)]
92. Lagarón, J.-M. Multifunctional and nanoreinforced polymers for food packaging. In *Multifunctional and Nanoreinforced Polymers for Food Packaging*; Elsevier: Amsterdam, The Netherlands, 2011; pp. 1–28.
93. Wang, J.; Zhang, H.; Wang, F.; Ai, X.; Huang, D.; Liu, G.; Mi, P. Enzyme-responsive polymers for drug delivery and molecular imaging. In *Stimuli Responsive Polymeric Nanocarriers for Drug Delivery Applications, Volume 1*; Elsevier: Amsterdam, The Netherlands, 2018; pp. 101–119.
94. Hung, L.X.; Bassène, P.D.; Thang, P.N.; Loan, N.T.; de Marcillac, W.D.; Dhawan, A.R.; Feng, F.; Esparza-Villa, J.U.; Hien, N.T.T.; Liem, N.Q. Near-infrared emitting CdTeSe alloyed quantum dots: Raman scattering, photoluminescence and single-emitter optical properties. *RSC Adv.* **2017**, *7*, 47966–47974. [[CrossRef](#)]
95. Valappil, M.O.; Pillai, V.K.; Alwarappan, S. Spotlighting graphene quantum dots and beyond: Synthesis, properties and sensing applications. *Appl. Mater. Today* **2017**, *9*, 350–371. [[CrossRef](#)]
96. Kleinman, S.L.; Frontier, R.R.; Henry, A.-I.; Dieringer, J.A.; Van Duyne, R.P. Creating, characterizing, and controlling chemistry with SERS hot spots. *Phys. Chem. Chem. Phys.* **2013**, *15*, 21–36. [[CrossRef](#)]
97. Nie, S.; Emory, S.R. Probing single molecules and single nanoparticles by surface-enhanced Raman scattering. *Science* **1997**, *275*, 1102–1106. [[CrossRef](#)]
98. Kneipp, K.; Wang, Y.; Kneipp, H.; Perelman, L.T.; Itzkan, I.; Dasari, R.R.; Feld, M.S. Single molecule detection using surface-enhanced Raman scattering (SERS). *Phys. Rev. Lett.* **1997**, *78*, 1667. [[CrossRef](#)]
99. Zhang, W.; Li, C.; Gao, K.; Lu, F.; Liu, M.; Li, X.; Zhang, L.; Mao, D.; Gao, F.; Huang, L. Surface-enhanced Raman spectroscopy with Au-nanoparticle substrate fabricated by using femtosecond pulse. *Nanotechnology* **2018**, *29*, 205301. [[CrossRef](#)]
100. Chang, T.-H.; Chang, Y.-C.; Chen, C.-M.; Chuang, K.-W.; Chou, C.-M. A facile method to directly deposit the large-scale Ag nanoparticles on a silicon substrate for sensitive, uniform, reproducible and stable SERS substrate. *J. Alloys Compd.* **2019**, *782*, 887–892. [[CrossRef](#)]
101. Wu, H.; Luo, Y.; Hou, C.; Huo, D.; Zhou, Y.; Zou, S.; Zhao, J.; Lei, Y. Flexible bipyramid-AuNPs based SERS tape sensing strategy for detecting methyl parathion on vegetable and fruit surface. *Sens. Actuators B Chem.* **2019**, *285*, 123–128. [[CrossRef](#)]
102. Fazio, E.; Neri, F.; Savasta, S.; Spadaro, S.; Trusso, S. Surface-enhanced Raman scattering of SnO₂ bulk material and colloidal solutions. *Phys. Rev. B* **2012**, *85*, 195423. [[CrossRef](#)]
103. Doğan, İ.; Gresback, R.; Nozaki, T.; van de Sanden, M. Analysis of temporal evolution of quantum dot surface chemistry by surface-enhanced Raman scattering. *Sci. Rep.* **2016**, *6*, 29508. [[CrossRef](#)]
104. Milekhin, A.G.; Sveshnikova, L.; Duda, T.; Surovtsev, N.V.; Adichtchev, S.; Zahn, D.R. Surface enhanced Raman scattering by CdS quantum dots. *JETP Lett.* **2008**, *88*, 799–801. [[CrossRef](#)]
105. Stadelmann, K.; Elizabeth, A.; Sabanés, N.M.; Domke, K.F. The SERS signature of PbS quantum dot oxidation. *Vib. Spectrosc.* **2017**, *91*, 157–162. [[CrossRef](#)]

106. Hugall, J.T.; Baumberg, J.J.; Mahajan, S. Surface-enhanced Raman spectroscopy of CdSe quantum dots on nanostructured plasmonic surfaces. *Appl. Phys. Lett.* **2009**, *95*, 141111. [[CrossRef](#)]
107. Lee, Y.-b.; Ho Lee, S.; Lee, S.; Lee, H.; Kim, J.; Joo, J. Surface enhanced Raman scattering effect of CdSe/ZnS quantum dots hybridized with Au nanowire. *Appl. Phys. Lett.* **2013**, *102*, 033109. [[CrossRef](#)]
108. Sheremet, E.; Milekhin, A.; Rodriguez, R.; Weiss, T.; Nesterov, M.; Rodyakina, E.; Gordan, O.; Sveshnikova, L.; Duda, T.; Gridchin, V. Surface-and tip-enhanced resonant Raman scattering from CdSe nanocrystals. *Phys. Chem. Chem. Phys.* **2015**, *17*, 21198–21203. [[CrossRef](#)] [[PubMed](#)]
109. Bak, S.; Kim, D.; Lee, H. Graphene quantum dots and their possible energy applications: A review. *Curr. Appl. Phys.* **2016**, *16*, 1192–1201. [[CrossRef](#)]
110. Panyathip, R.; Sucharitakul, S.; Phaduangdhitidhada, S.; Ngamjarurojana, A.; Kumnorkaew, P.; Choopun, S. Surface Enhanced Raman Scattering in Graphene Quantum Dots Grown via Electrochemical Process. *Molecules* **2021**, *26*, 5484. [[CrossRef](#)] [[PubMed](#)]
111. Ostrovskaya, L.Y. Characterization of different carbon nanomaterials promising for biomedical and sensor applications by the wetting method. *Powder Metall. Met. Ceram.* **2003**, *42*, 1–8. [[CrossRef](#)]
112. Ling, X.; Xie, L.; Fang, Y.; Xu, H.; Zhang, H.; Kong, J.; Dresselhaus, M.S.; Zhang, J.; Liu, Z. Can graphene be used as a substrate for Raman enhancement? *Nano Lett.* **2010**, *10*, 553–561. [[CrossRef](#)] [[PubMed](#)]
113. Gulzar, A.; Yang, P.; He, F.; Xu, J.; Yang, D.; Xu, L.; Jan, M.O. Bioapplications of graphene constructed functional nanomaterials. *Chem. -Biol. Interact.* **2017**, *262*, 69–89. [[CrossRef](#)]
114. Kumar, S.; Tokunaga, K.; Namura, K.; Fukuoka, T.; Suzuki, M. Experimental evidence of a twofold electromagnetic enhancement mechanism of surface-enhanced Raman scattering. *J. Phys. Chem. C* **2020**, *124*, 21215–21222. [[CrossRef](#)]
115. Lu, Y.; Lin, L.; Ye, J. Human metabolite detection by surface-enhanced Raman spectroscopy. *Mater. Today Bio* **2022**, *13*, 100205. [[CrossRef](#)]
116. Pearson, B.; Wang, P.; Mills, A.; Pang, S.; McLandsborough, L.; He, L. Innovative sandwich assay with dual optical and SERS sensing mechanisms for bacterial detection. *Anal. Methods* **2017**, *9*, 4732–4739. [[CrossRef](#)]
117. Fateixa, S.; Nogueira, H.I.; Trindade, T. Hybrid nanostructures for SERS: Materials development and chemical detection. *Phys. Chem. Chem. Phys.* **2015**, *17*, 21046–21071. [[CrossRef](#)]
118. Sharma, B.; Frontiera, R.R.; Henry, A.-I.; Ringe, E.; Van Duyne, R.P. SERS: Materials, applications, and the future. *Mater. Today* **2012**, *15*, 16–25. [[CrossRef](#)]
119. Ngo, H.T.; Wang, H.-N.; Fales, A.M.; Vo-Dinh, T. Plasmonic SERS biosensing nanochips for DNA detection. *Anal. Bioanal. Chem.* **2016**, *408*, 1773–1781. [[CrossRef](#)] [[PubMed](#)]
120. Ganesh, S.; Venkatakrisnan, K.; Tan, B. Quantum scale organic semiconductors for SERS detection of DNA methylation and gene expression. *Nat. Commun.* **2020**, *11*, 1135. [[CrossRef](#)] [[PubMed](#)]
121. Saviñon-Flores, F.; Méndez, E.; López-Castaños, M.; Carabarin-Lima, A.; López-Castaños, K.A.; González-Fuentes, M.A.; Méndez-Albores, A. A review on SERS-based detection of human virus infections: Influenza and coronavirus. *Biosensors* **2021**, *11*, 66. [[CrossRef](#)]
122. Rajender, G.; Giri, P. Formation mechanism of graphene quantum dots and their edge state conversion probed by photoluminescence and Raman spectroscopy. *J. Mater. Chem. C* **2016**, *4*, 10852–10865. [[CrossRef](#)]
123. Aronson, J.K. Biomarkers and surrogate endpoints. *Br. J. Clin. Pharmacol.* **2005**, *59*, 491. [[CrossRef](#)] [[PubMed](#)]
124. Tanaka, T.; Tanaka, M.; Tanaka, T.; Ishigamori, R. Biomarkers for colorectal cancer. *Int. J. Mol. Sci.* **2010**, *11*, 3209–3225. [[CrossRef](#)]
125. Vaughan, L. Biomarkers in acute medicine. *Medicine* **2017**, *45*, 150–156. [[CrossRef](#)]
126. Mousavi, S.M.; Low, F.W.; Hashemi, S.A.; Lai, C.W.; Ghasemi, Y.; Soroshnia, S.; Savardashtaki, A.; Babapoor, A.; Pynadathu Rumjit, N.; Goh, S.M. Development of graphene based nanocomposites towards medical and biological applications. *Artif. Cells Nanomed. Biotechnol.* **2020**, *48*, 1189–1205. [[CrossRef](#)]
127. McCormick, T.; Martin, K.; Hehenberger, M. *The Evolving Role of Biomarkers: Focusing on Patients from Research to Clinical Practice*; IBM Global Business Services: Pyrmont, NSW, Australia, 2007; Volume 4, pp. 1–20.
128. Mayeux, R. Biomarkers: Potential uses and limitations. *NeuroRx* **2004**, *1*, 182–188. [[CrossRef](#)]
129. Gârban, Z.; Avacovici, A.; Gârban, G.; Ghibu, G.; Velciov, A.B.; Pop, C.I. Biomarkers: Theoretical aspects and applicative peculiarities note i. general characteristics of biomarkers. *Agroalim. Process Technol* **2005**, *11*, 139–146.
130. Hashemi, S.A.; Mousavi, S.M.; Faghihi, R.; Arjmand, M.; Rahsepar, M.; Bahrani, S.; Ramakrishna, S.; Lai, C.W. Superior X-ray radiation shielding effectiveness of biocompatible polyaniline reinforced with hybrid graphene oxide-iron tungsten nitride flakes. *Polymers* **2020**, *12*, 1407. [[CrossRef](#)] [[PubMed](#)]
131. Polivka, J.; Krakorova, K.; Peterka, M.; Topolcan, O. Current status of biomarker research in neurology. *EPMA J.* **2016**, *7*, 14. [[CrossRef](#)] [[PubMed](#)]
132. Tietjen, G.E.; Khubchandani, J. Vascular biomarkers in migraine. *Cephalalgia* **2015**, *35*, 95–117. [[CrossRef](#)]
133. Tietjen, G.E.; Khubchandani, J.; Herial, N.A.; Shah, K. Adverse childhood experiences are associated with migraine and vascular biomarkers. *Headache: J. Head Face Pain* **2012**, *52*, 920–929. [[CrossRef](#)]
134. Durham, P.; Papapetropoulos, S. Biomarkers associated with migraine and their potential role in migraine management. *Headache J. Head Face Pain* **2013**, *53*, 1262–1277. [[CrossRef](#)]

135. Hashemi, S.A.; Mousavi, S.M.; Naderi, H.R.; Bahrani, S.; Arjmand, M.; Hagfeldt, A.; Chiang, W.-H.; Ramakrishna, S. Reinforced polypyrrole with 2D graphene flakes decorated with interconnected nickel-tungsten metal oxide complex toward superiorly stable supercapacitor. *Chem. Eng. J.* **2021**, *418*, 129396. [[CrossRef](#)]
136. Ishizaki, K.; Takeshima, T.; Fukuhara, Y.; Araki, H.; Nakaso, K.; Kusumi, M.; Nakashima, K. Increased plasma transforming growth factor- β 1 in migraine. *Headache J. Head Face Pain* **2005**, *45*, 1224–1228. [[CrossRef](#)]
137. Kurth, T.; Ridker, P.; Buring, J. Migraine and biomarkers of cardiovascular disease in women. *Cephalalgia* **2008**, *28*, 49–56. [[CrossRef](#)]
138. Song, C.; Guo, S.; Jin, S.; Chen, L.; Jung, Y.M. Biomarkers determination based on surface-enhanced Raman scattering. *Chemosensors* **2020**, *8*, 118. [[CrossRef](#)]
139. Li, Y.; Liu, X.; Guo, J.; Zhang, Y.; Guo, J.; Wu, X.; Wang, B.; Ma, X. Simultaneous detection of inflammatory biomarkers by SERS nanotag-based lateral flow assay with portable cloud Raman spectrometer. *Nanomaterials* **2021**, *11*, 1496. [[CrossRef](#)] [[PubMed](#)]
140. Ranjan, R.; Esimbekova, E.N.; Kratasyuk, V.A. Rapid biosensing tools for cancer biomarkers. *Biosens. Bioelectron.* **2017**, *87*, 918–930. [[CrossRef](#)]
141. Chen, R.; Du, X.; Cui, Y.; Zhang, X.; Ge, Q.; Dong, J.; Zhao, X. Vertical flow assay for inflammatory biomarkers based on nanofluidic channel array and SERS nanotags. *Small* **2020**, *16*, 2002801. [[CrossRef](#)]
142. Liu, H.; Gao, X.; Xu, C.; Liu, D. SERS Tags for Biomedical Detection and Bioimaging. *Theranostics* **2022**, *12*, 1870. [[CrossRef](#)] [[PubMed](#)]
143. Singh, S.; Deshmukh, A.; Chaturvedi, P.; Krishna, C.M. In vivo Raman spectroscopic identification of premalignant lesions in oral buccal mucosa. *J. Biomed. Opt.* **2012**, *17*, 105002. [[CrossRef](#)] [[PubMed](#)]
144. Hamza, T.H.; Zabetian, C.P.; Tenesa, A.; Laederach, A.; Montimurro, J.; Yearout, D.; Kay, D.M.; Doheny, K.F.; Paschall, J.; Pugh, E. Common genetic variation in the HLA region is associated with late-onset sporadic Parkinson's disease. *Nat. Genet.* **2010**, *42*, 781–785. [[CrossRef](#)]
145. Araujo, D.; Lapchak, P. Induction of immune system mediators in the hippocampal formation in Alzheimer's and Parkinson's diseases: Selective effects on specific interleukins and interleukin receptors. *Neuroscience* **1994**, *61*, 745–754. [[CrossRef](#)]
146. Maddon, P.J.; Dalgleish, A.G.; McDougal, J.S.; Clapham, P.R.; Weiss, R.A.; Axel, R. The T4 gene encodes the AIDS virus receptor and is expressed in the immune system and the brain. *Cell* **1986**, *47*, 333–348. [[CrossRef](#)]
147. Maffia, P.; Zinselmeyer, B.H.; Ialenti, A.; Kennedy, S.; Baker, A.H.; McInnes, I.B.; Brewer, J.M.; Garside, P. Images in cardiovascular medicine: Multiphoton microscopy for three-dimensional imaging of lymphocyte recruitment into apolipoprotein-E-deficient mouse carotid artery. *Circulation* **2007**, *115*, e326–e328. [[CrossRef](#)]
148. Gabriel, S.E. The epidemiology of rheumatoid arthritis. *Rheum. Dis. Clin. N. Am.* **2001**, *27*, 269–281. [[CrossRef](#)]
149. Ortolano, F.; Maffia, P.; Dever, G.; Hutchison, S.; Benson, R.; Millington, O.; De Simoni, M.; Bushell, T.; Garside, P.; Carswell, H. Imaging T-cell movement in the brain during experimental cerebral malaria. *Parasite Immunol.* **2009**, *31*, 147–150. [[CrossRef](#)]
150. Fumagalli, S.; Coles, J.A.; Ejlerskov, P.; Ortolano, F.; Bushell, T.J.; Brewer, J.M.; De Simoni, M.-G.; Dever, G.; Garside, P.; Maffia, P. In vivo real-time multiphoton imaging of T lymphocytes in the mouse brain after experimental stroke. *Stroke* **2011**, *42*, 1429–1436. [[CrossRef](#)] [[PubMed](#)]
151. Theer, P.; Denk, W. On the fundamental imaging-depth limit in two-photon microscopy. *JOSA A* **2006**, *23*, 3139–3149. [[CrossRef](#)] [[PubMed](#)]
152. Zipfel, W.R.; Williams, R.M.; Christie, R.; Nikitin, A.Y.; Hyman, B.T.; Webb, W.W. Live tissue intrinsic emission microscopy using multiphoton-excited native fluorescence and second harmonic generation. *Proc. Natl. Acad. Sci. USA* **2003**, *100*, 7075–7080. [[CrossRef](#)]
153. Patterson, G.H.; Piston, D.W. Photobleaching in two-photon excitation microscopy. *Biophys. J.* **2000**, *78*, 2159–2162. [[CrossRef](#)]
154. König, K. Multiphoton microscopy in life sciences. *J. Microsc.* **2000**, *200*, 83–104.
155. McQueenie, R.; Stevenson, R.; Benson, R.; MacRitchie, N.; McInnes, I.; Maffia, P.; Faulds, K.; Graham, D.; Brewer, J.; Garside, P. Detection of inflammation in vivo by surface-enhanced Raman scattering provides higher sensitivity than conventional fluorescence imaging. *Anal. Chem.* **2012**, *84*, 5968–5975. [[CrossRef](#)]
156. Zavaleta, C.L.; Smith, B.R.; Walton, I.; Doering, W.; Davis, G.; Shojaei, B.; Natan, M.J.; Gambhir, S.S. Multiplexed imaging of surface enhanced Raman scattering nanotags in living mice using noninvasive Raman spectroscopy. *Proc. Natl. Acad. Sci. USA* **2009**, *106*, 13511–13516.
157. Maiti, K.K.; Dinish, U.; Fu, C.Y.; Lee, J.-J.; Soh, K.-S.; Yun, S.-W.; Bhuvaneshwari, R.; Olivo, M.; Chang, Y.-T. Development of biocompatible SERS nanotag with increased stability by chemisorption of reporter molecule for in vivo cancer detection. *Biosens. Bioelectron.* **2010**, *26*, 398–403.